Electronic Supplementary Material (ESI) for Nanoscale.

This ESI replaces the original version published on 16 Jan 2024

Supporting Information

Electroosmotic Flows Spin Tracers Near Chemical Nano/Micromotors

Donghao Cui[1], Zuyao Yan[1], Xiaowen Chen[1], Jiayu Liu[1], Wei Wang[1*]

1. School of Materials Science and Engineering, Harbin Institute of Technology (Shenzhen), Shenzhen, Guangdong, 518055, China

Corresponding author: Wei Wang (weiwangsz@hit.edu.cn)

1. Experimental details

1.1 Synthesis of nanorods and Janus microspheres

Preparation of nanorods. Nanorods were synthesized utilizing the method previously reported.[1] Anodized alumina film (AAO, purchased from Whatman, 200 nm nominal pore diameter) was used as the template for metal electrodeposition. To serve as the working electrode, a 100 nm silver layer was evaporated on the back of the AAO membrane using the HHV TF500 electron beam evaporation system. To conceal the branched channels at the bottom of the AAO template, a sacrificial layer of Ag was deposited before Au and Rh. A two-electrode system with a platinum coil as both the counter-electrode and the reference electrode was implemented. A typical experiment involved initial electrodeposition of the sacrificial Ag layer for 3000 s in the AAO membrane at a current density of -1.02 mA/cm^2. The deposition of Au and Rh at current density of 0.20 mA/cm^2 and 1.02 mA/cm^2, respectively. The length of two metals in the rod can be controlled by the deposition time. Pure Au nanorod tracers were synthesized following the same protocol without plating Rh. The Au plating solution was home-made, while the Ag and Rh plating solutions were purchased from Alfa Aesar (#44067) and Technic Inc (#290255GL), respectively. To eliminate the Ag layer utilized for conduction and masking, the AAO membrane was submerged in dilute HNO_3 aqueous solution for 0.5 h and subsequently rinsed with deionized water.

Preparation of Janus microspheres. Janus microspheres such as SiO_2-Au, Au-Pt, SiO_2-Au and TiO_2-Pt were fabricated by depositing a metal layer on top of the corresponding microspheres. The process for SiO_2-Au is described below. SiO_2 microspheres with a diameter of 2 μm, purchased from Tianjin Baseline Chrometch Research Center, were suspended in ethanol and drop-casted onto a pre-cleaned glass slide to prepare a monolayer. A 20 nm gold layer was then coated onto the monolayer of SiO_2 via a low vacuum sputter-coater (model SBC-12, KYKY). The resulting SiO_2-Au Janus microparticles were released from the glass slides by ultrasonication and resuspended in deionized water. Gold microspheres were chemically synthesized following the procedure in reference 2,[2] and microspheres of different sizes were separated by centrifugation. TiO_2 microspheres were synthesized chemically following the procedure in reference 3,[3] by coating commercial SiO_2 microspheres with a thin TiO_2 shell.

1.2 Motor experiment

All particles used in the experiment were dispersed in deionized water prior to use. The motor suspension and Janus tracer were both dropped on a glass slide, and the solution of H_2O_2 (Alfa Aesar #33323) was added dropwise using pipettes until the desired concentration was reached. The behavior of particles was observed using an inverted optical microscope (Olympus IX73). Videos were captured by a Point Grey camera (FL3-U3-13E4C-C) mounted on the microscope typically at 15 frames per second. MATLAB codes provided by Prof. Hepeng Zhang at Shanghai Jiaotong University were used to process and analyze the videos. Motor speeds were calculated by dividing the displacement between two frames by the time interval between them (0.067 s).

2. COMSOL simulation details

2.1 Self-electrophoresis model of the Au-Rh nanorod

The COMSOL Multiphysics package (version 5.4) was used to create two 3D models for simulating the electric and fluid fields surrounding the Au-Rh nanorod and the tracer in its vicinity (see Figure S1 and S2 for geometric configurations). The dimensions of the nanorod were fixed at 3 μm length and 300 nm diameter in both models, while the tracer sphere had a diameter of 2 μm. The rod and the sphere was separated by 100 nm. The nanorods were placed in the center of a cube box of dimensions 50 μm, filled with water of a pH of 5.6, to mimic a realistic solution environment saturated with CO_2.

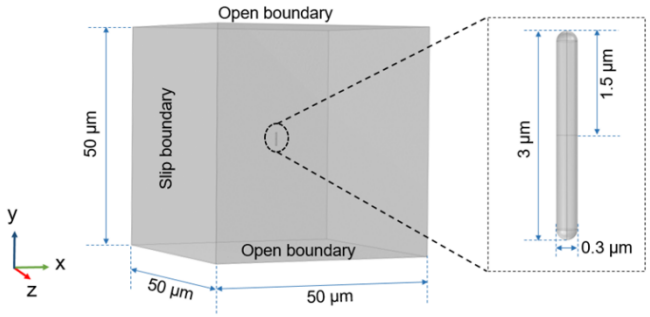

Figure S1 Schematic of an Au-Rh nanorod in COMSOL.

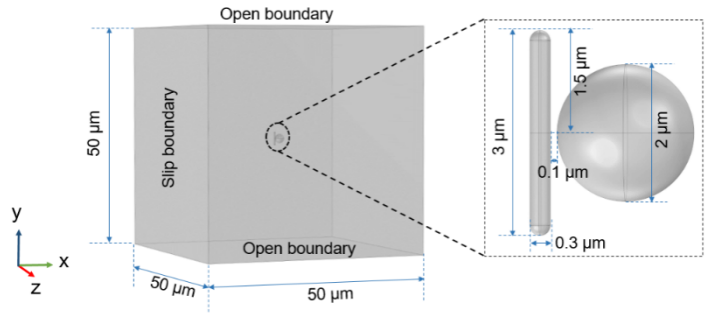

Figure S2 Schematic diagram of an Au-Rh nanorod with an inert microsphere in COMSOL.

Since the Au-Rh nanorods move via self-electrophoresis, the oxidation and reduction of H_2O_2 occur preferentially at the Rh and the Au ends, respectively, resulting in the production and consumption of protons. Based on the previous work,[4,5] the anode or cathode with an outward or inward flux of protons can be regard as carrying a surface charge of ρ_a and ρ_c in the electrostatic module, respectively:

$$\rho_{\mathrm{a}} = \varepsilon E_{\mathrm{a}} = \varepsilon \frac{J_a \mathrm{k_B} T}{2 e n_0 \mathrm{D_{H^+}}};\ \rho_{\mathrm{c}} = \varepsilon E_{\mathrm{c}} = \varepsilon \frac{J_c \mathrm{k_B} T}{2 e n_0 \mathrm{D_{H^+}}} \qquad \text{Eqn.S1}$$

where ε is the medium electrical permittivity, n_0 is the bulk proton concentration, J_a and J_c are the ionic flux on anode and cathode, and D_{H^+} is the diffusivities of H^+. In addition, we set the electrical potential at the boundary of the box to be zero since protons are not produced and consumed there.
The values used in calculating ρ are listed in Table S1.

Table S1 Parameters for calculating ρ

Parameter	Note	Value
J_a	Proton flux on the anode	7×10^{-6} mol/(m²·s)
J_c	Proton flux on the cathode	-7×10^{-6} mol/(m²·s)
T	Temperature	293.15 K
D_{H^+}	Diffusivities of H^+	9.311×10^{-9} m²/s
n_0	Bulk proton concentration	2.5×10^{-3} mol/m³

The surface charge density was calculated to be 2.7×10^{-9} C/m².
In the creeping flow module, the top and the bottom surface of the box were set to be open boundaries for the flow, while all side walls were set to be slip boundaries (no stress). The fluid was set as incompressible flow to simulate the Stokes flow. No slip condition was set on the microsphere surface. Electroosmotic boundary condition was set on the nanorods surface:

$$\boldsymbol{v} = \frac{\zeta \varepsilon}{\mu} \boldsymbol{E} \qquad \text{Eqn.S2}$$

where v is the electroosmotic speed of fluid on the nanorod surface, ζ is the zeta potential on the nanorod surface (set to be -47 mV[6]), and E is the tangential component of the electric field that is solved by Eqn. S1.

2.2 Simulation of the Au-Rh nanorod collecting the tracer

The distribution of potential and field strength around the nanorod is shown in the Figure.S3 based on the above model. The solutions near the two ends of the rod are positive and negatively charged, respectively, so that negatively charged tracers migrate toward the anode via electrophoresis. The field strength is very large at the metal junction of a nanorod, and causes dielectrophoresis of tracers that are more polarizable than water. The magnitude of the DEP force F_{DEP}, whether positive or negative, of a sphere is given by,[7]

$$\boldsymbol{F_{DEP}} = 4\pi\varepsilon R^3 \mathrm{Re}(K) \nabla \boldsymbol{E}^2 \qquad \text{Eqn.S3}$$

where R is the microsphere radius, Re(K) is the real component polarizability of the Clausius-Mossotti factor K (related to the electrical polarizability of the particle), and E is the electric field strength.

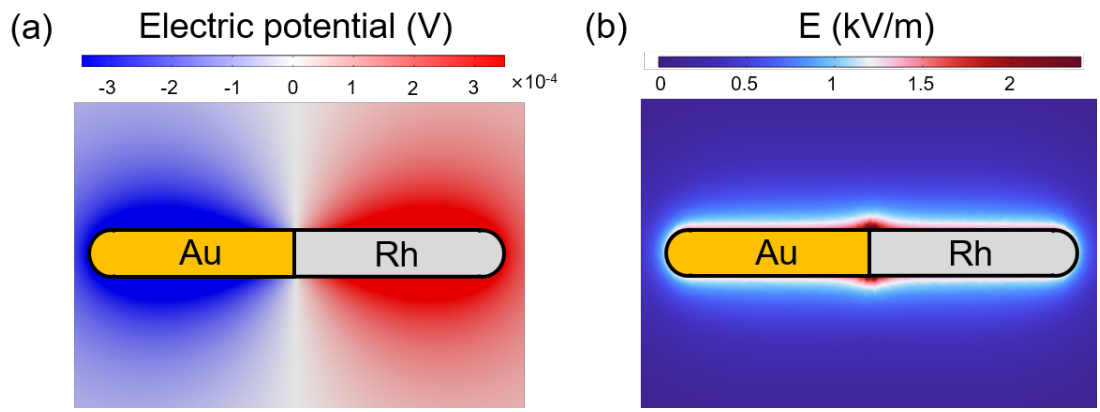

Figure S3 The distributions of electrical potential and modulus of field strength around the nanorod on the xy plane. (a): electrical potential. (b): the magnitude of electric field strength

The real component of the Claussius-Mossotti factor, Re(K), can be solved by taking the real part of the following:

$$K = \frac{\varepsilon_p^* - \varepsilon_m^*}{\varepsilon_p^* + 2\varepsilon_m^*} \qquad \text{Eqn.S4}$$

$$\varepsilon_p^* = \varepsilon_p - \mathrm{i}\frac{\sigma_p}{\omega}; \qquad \varepsilon_m^* = \varepsilon_m - \mathrm{i}\frac{\sigma_m}{\omega} \qquad \text{Eqn.S5}$$

where ε_m and ε_p are the dielectric permittivity of the media and the particle, respective, and σ_m and σ_p are their electrical conductivity. ω is the driving frequency of the oscillating electric field. The σ_m of a 1:1 electrolyte of valence of Z is :

$$\sigma_m = \sigma_m^+ + \sigma_m^- = \frac{z^2 e^2 N_A c_0}{k_B T}(D^+ + D^-) \qquad \text{Eqn.S6}$$

where + and – correspond to the cation and ion, respectively, and D is the ion diffusivity. c_0 is the ion concentration in the bulk, and N_A is the Avogadro number.

The σ_p of dielectric particle of radius, R is sum of its bulk conductivity σ_b and surface conductivity σ_s the latter of which is further composed of the conductivity of Stern layer (K_{sl}) and that of the diffuse layer (K_d).[8–10]

$$\sigma_p = \sigma_b + (K_{sl} + K_d)/R \qquad \text{Eqn.S7}$$

$$K_\mathrm{d} = \frac{2\sigma_\mathrm{m}}{\kappa}\left\{\begin{array}{l} \dfrac{D^+}{D^+ + D^-}\left[\exp\left(-\dfrac{\mathrm{Z}\tilde{\zeta}}{2}\right) - 1\right](1 + 3m^+) \\ + \dfrac{D^-}{D^+ + D^-}\left[\exp\left(+\dfrac{\mathrm{Z}\tilde{\zeta}}{2}\right) - 1\right](1 + 3m^-) \end{array}\right\} \qquad \text{Eqn.S8}$$

$$\tilde{\zeta} = \frac{\mathrm{e}}{k_\mathrm{B}T}\zeta_\mathrm{p} \qquad \text{Eqn.S9}$$

$$m^\pm = \frac{2\varepsilon_\mathrm{m}}{3\eta D^\pm}\left(\frac{k_\mathrm{B}T}{\mathrm{Ze}}\right)^2 \qquad \text{Eqn.S10}$$

$$\kappa^{-1} = \lambda_\mathrm{D} = \sqrt{\frac{\varepsilon_\mathrm{m} k_\mathrm{B} T}{2\mathrm{Z}^2 \mathrm{e}^2 n_0}} \qquad \text{Eqn.S11}$$

where ζ_p is the zeta potential of the particle, and κ^{-1} is the characteristic length of the electrical double layer (also known as the Debye length, λ_D). Ksl, on the other hand, is typically assigned, and we have chosen a value of 5×10^{-9} S, well within the common range used in the literature.[11]

The values used in calculating Re(K) are listed in Table S2.

Table S2 Parameters for calculating Re(K)

Parameter	Note	Value
T	Temperature	293.15 K
ζ_p	Particle zeta potential	SiO_2 sphere: -46 mV[12] Au sphere: -64 mV[6]
ε_m	Electrical permittivity of water	$78.5\varepsilon_0$
ε_p	Electrical permittivity of polystyrene	$3.4\varepsilon_0$
D^+	Diffusivity of H^+	9.3×10^{-9} $m^2\cdot s^{-1}$
D^-	Diffusivity of HCO_3^-	1.1×10^{-9} $m^2\cdot s^{-1}$
η	Dynamic viscosity of water at 293.15 K	1.0016×10^{-3} $Pa\cdot s^{-1}$
σ_b	Bulk conductivity of silica	1×10^{-10} $S\cdot m^{-1}$[13]
K_{sl}	Stern layer conductivity	5×10^{-9} S

Following the above equations, the Re(k) of a 1 μm SiO_2 microsphere is calculated to be 0.95, and the Re(k) of a 1 μm gold microsphere is 1, both of which exhibit positive dielectrophoresis. Therefore, it is inferred that the SiO_2-Au Janus microspheres used in the experiment also undergo positive dielectrophoresis.

2.3 Simulation of the torque on the spinning tracer

Affected by the Au-Rh nanorod, the tracer spun due to electrophoresis and electroosmotic flow on surface. The torque generated by either is calculated separately in this section, based on the COMSOL models described in 2.1.
The contribution of the force at a point (x, y) to the torque of disk is shown in Fig. S12 by the Eqn. S12,

$$\boldsymbol{M}_{disk} = \boldsymbol{F}_x(y - y_0) - \boldsymbol{F}_y(\boldsymbol{x} - \boldsymbol{x}_0) \qquad \text{Eqn.S12}$$

where M_{disk} is the torque on the disk (clockwise is positive), F_x and F_y are the force on this point (x, y) from the x and y direction, (x_0, y_0) is the coordinate of the center of mass of the disk (Fig. S4).

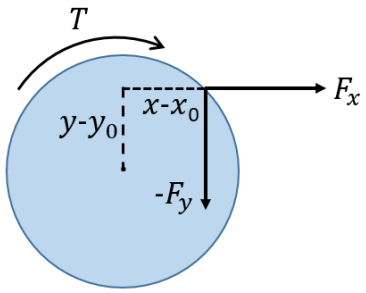

Figure S4 Schematic diagram of calculating the torque generated by a point on the disc

Therefore, for a sphere subjected to an external stress, the torque on the xy plane can be calculated by the Eqn. S13,

$$\boldsymbol{M}_{\text{sphere}} = \oint_S \boldsymbol{T}_x(y - y_0) - \boldsymbol{T}_y(x - x_0)\ dS \qquad \text{Eqn.S13}$$

where M_{sphere} is the torque on the sphere on xy plane (clockwise is positive), T_x and T_y are the stress components, (x_0, y_0) is the coordinate of the center of the sphere.

Because the stress on the particle is opposite to the stress on the fluid around the particle, the torque caused by electroosmotic flow can be calculated by the Eqn. S14,

$$\boldsymbol{M}_{\text{fluid}} = \oint_S (-\boldsymbol{T}_{fluidx})(y - y_0) - (-\boldsymbol{T}_{fluidy})(x - x_0)\ dS \qquad \text{Eqn.S14}$$

where T_{fluidx} and T_{fluidy} are the x and y stress components on the fluid at the point (x,y) from the x and y direction, obtained from the Laminar flow module in COMSOL.

Because the electrophoretic stress can be expressed as the product of surface charge density and field strength, the torque caused by electrophoretic forces can be calculated by Eqn. S15,

$$\boldsymbol{M}_{\text{ele}} = \oint_S \boldsymbol{E_x}\rho_s(y - y_0) - \boldsymbol{E_y}\rho_s(x - x_0)\ dS \qquad \text{Eqn.S15}$$

where E_x and E_y are the field strength components obtained from the Electrostatics module in COMSOL, ρ_s is the surface charge density of the SiO_2 tracer microsphere:

$$\rho_s = \varepsilon\kappa\varphi_0\left(\frac{1+\kappa a}{\kappa a}\right) \quad \text{Eqn.S16}$$

where φ_0 is the surface potential of tracer (approximated by its zeta potential as -46 mV[12]), a = 1×10^{-6} m is the radius of the tracer.

2.4 Simulation of the three-dimensionally spinning near substrate

The particles and the substrate are both negatively charged in the water, so the resulting electrostatic repulsion will balance the gravity of the particles and keep them suspended at a certain height from the substrate, the expression is shown as follow:[14]

$$\kappa B exp(-\kappa h) = -\frac{4}{3}\pi a^3(\rho_P - \rho_f)g \quad \text{Eqn.S17}$$

$$B = 64\pi\varepsilon a(\frac{k_B T}{e})^2 \tanh(\frac{e\zeta_s}{4kT})\tanh(\frac{e\zeta_p}{4kT}) \quad \text{Eqn.S18}$$

where h is the suspension height of the particle, ρ_p and ρ_f are the densities of water and particles, ζ_s and ζ_p are the zeta potential of substrate and particles.
The values used in calculating h are listed in Table S3.

Table S3 Parameters for calculating h

Parameter	Note	Value
T	Temperature	293.15 K
ζ_p	Tracer zeta potential	tracer: -46 mV[12], rod: -47mV[6]
ζ_s	Substrate zeta potential	-73 mV[12]
ρ_f	Density of water	1×10^3 kg/m^3
ρ_t	Density of silica	2.2×10^3 kg/m^3
ρ_r	Density of Au	19.3×10^3 kg/m^3
a_t	Radius of tracer	1×10^{-6} m
a_r	Radius of nanorod	1.5×10^{-7} m

For silica tracers, the suspension height is calculated to be h_t = 0.45 μm based on the balance between the electrostatic repulsion and the gravitational force. The Au-Rh nanorods can be regard as a long chain of gold spheres of the same diameter, from which the calculated suspension height is h_r = 0.60 μm. The new 3D model of the particles near the substrate was constructed based on the above height data, see Fig.S5.

The resulting fluid torque is -1.67×10^{-19} N·m on the xy plane, -8.13×10^{-23} N·m on the xz plane, and 1.12×10^{-19} N·m on the yz plane, corresponding to the spinning speed of 1 rps on the xy plane and 0.67 rps on the yz plane, which is similar to the 3D spinning observed in the experiment as 0.73 on the xy plane and 0.58 rps on the yz plane. The fluid field on the xy and yz planes (See Fig.S6) is consistent with the three-dimensional rotation observed in the experiment.

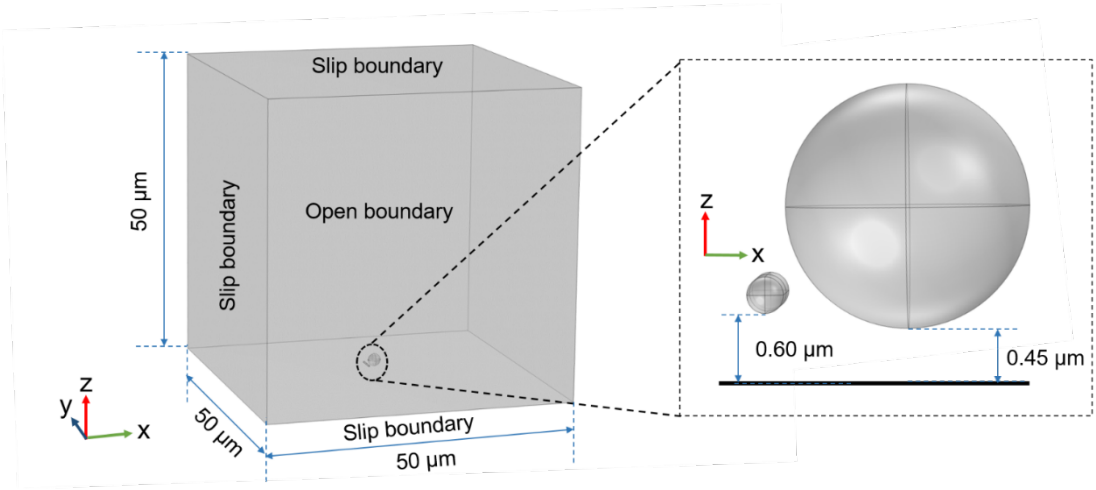

Figure S5 Schematic diagram of an Au-Rh nanorod with a inert microsphere near substrate in COMSOL

3. Supplementary Figures

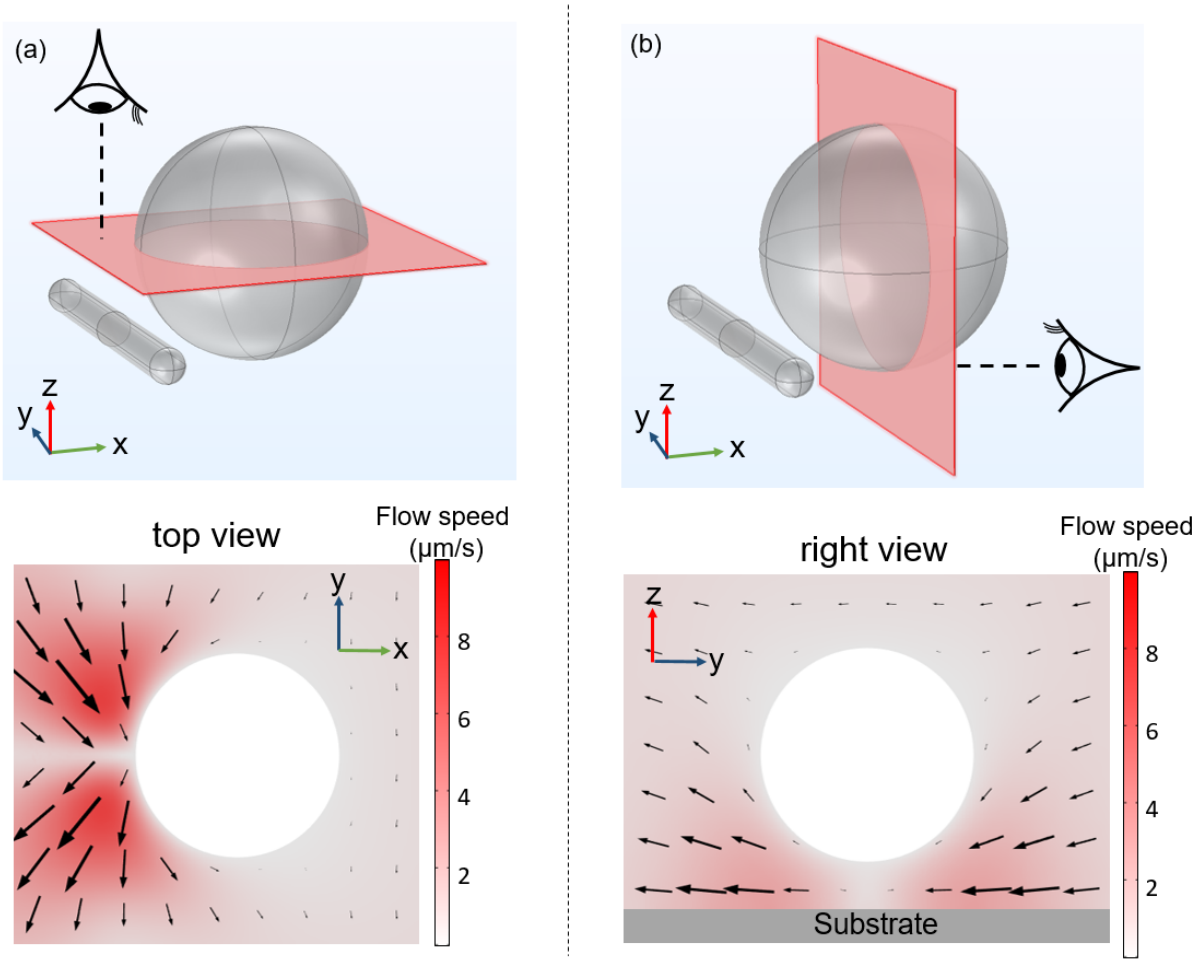

Figure S6 Simulated flow fields on the xy (a) and yz (b) cut planes shown in the top figures.

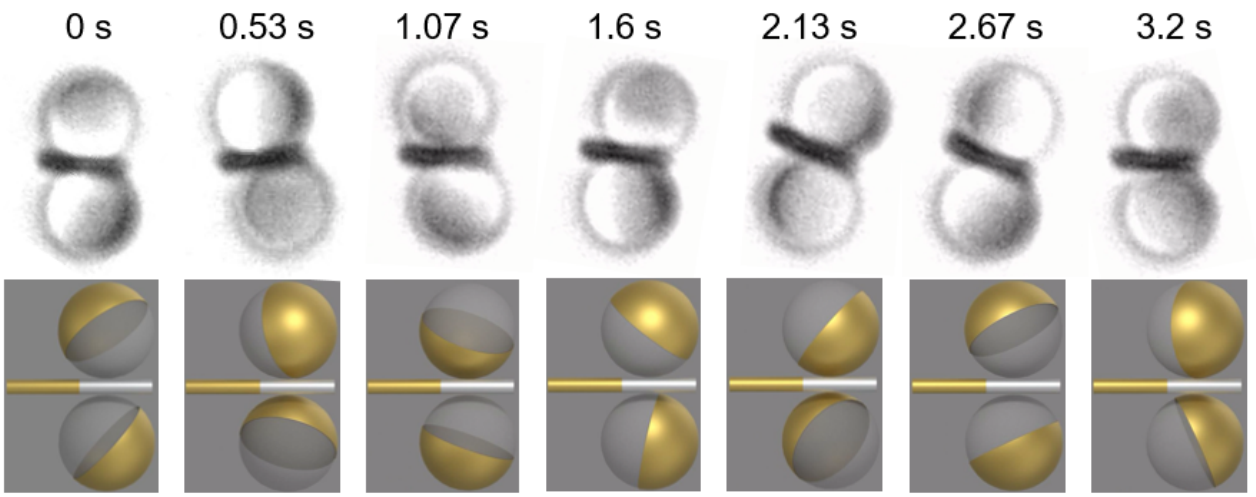

Figure S7 Optical micrographs (top) and cartoons (bottom) of two SiO_2-Au Janus microspheres spinning in 3D next to a Au-Rh nanorod motor.

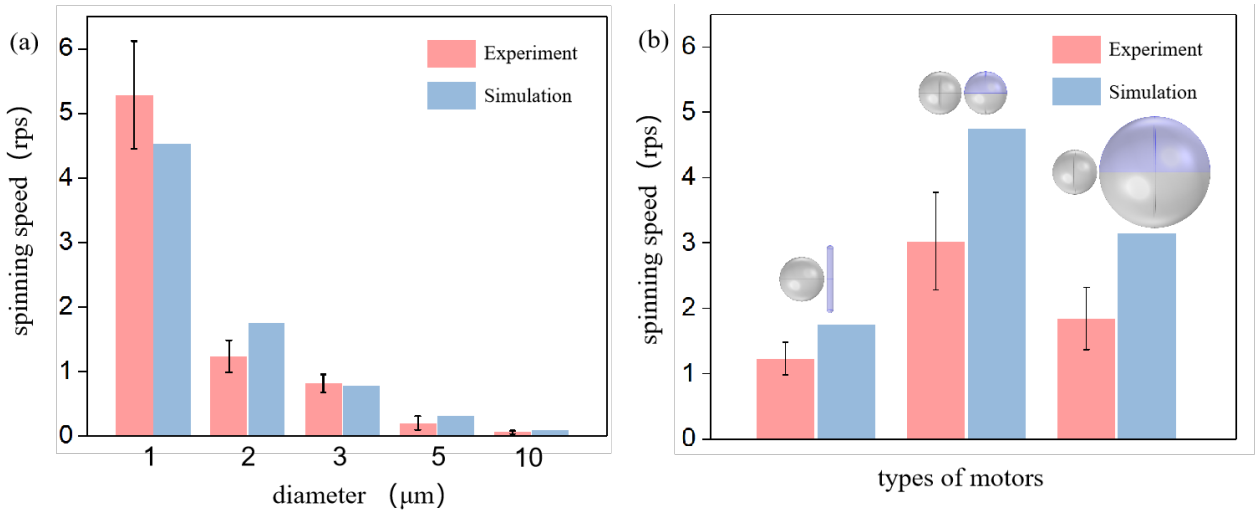

Figure S8 The spinning speed of (a) tracers of different sizes and (b) motors of different types in experiments and simulations

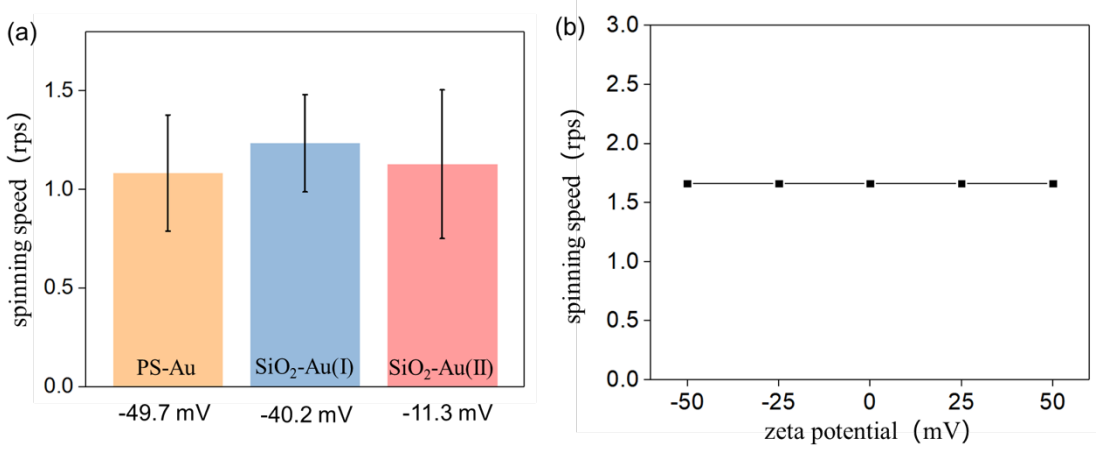

Figure S9 The spinning speed of tracers of different zeta potential in (a) experiments and (b) simulations. The two SiO_2-Au Janus spheres were fabricated by the same method but from SiO_2 spheres of different vendors, leading to different surface zeta potential.

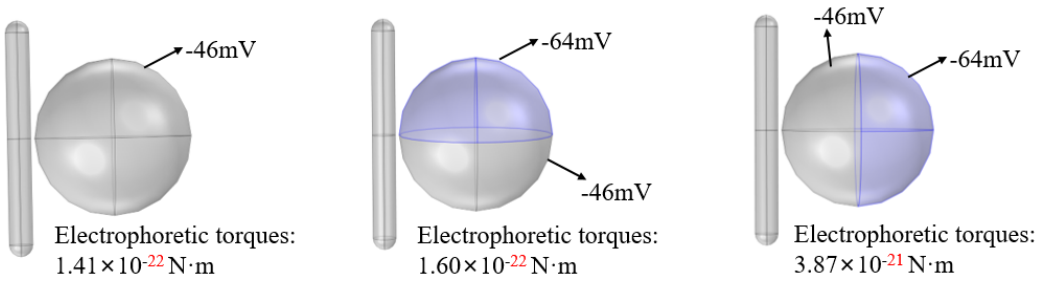

Figure S10. Simulated torques for microspheres of three different charge distributions.

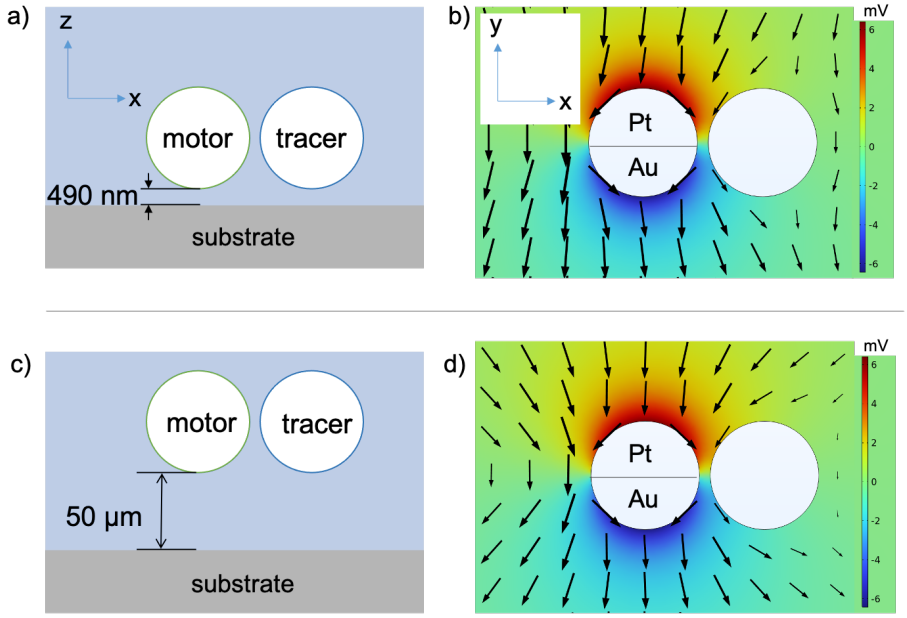

Figure S11. The effect of bottom substrate on the spinning of tracers on the xy plane. (a, b): schematic (a) and numerical simulation (b) of a pair of Au-Pt spherical micromotor and a microsphere tracer 490 nm above a charged substrate. See Supporting Information for estimate for their heights. (c, d) are the same as (a, b) except that both particles are placed far (50 μm) above the substrate. Colors represent electrical potential and arrows correspond to flows in (b) and (d). Parameters used in (b) and (d) are given in the Supporting Information.

4.Supplementary videos

Videos are played at the original speed unless otherwise noted. All experiments shown in the videos were conducted in H_2O_2 aqueous solution. (Video S1-S5 are in 10 wt% H_2O_2, Video S6-S7 are in 5 wt% H_2O_2)

Video S1: SiO_2-Au Janus microspheres spinning in 3D near Au-Rh nanorods.

Video S2: One SiO_2-Au Janus microsphere spinning next to a Au-Rh nanorod on the xy plane.

Video S3: One Au-Rh nanorod collecting and spinning multiple SiO_2-Au Janus microspheres sequentially.

Video S4: A tracer Au nanorod swinging during the passage of a nearby Au-Rh nanorod.

Video S5: Au-Rh nanorods spinning SiO_2-Au Janus microspheres of two sizes.

Video S6: SiO_2-Pt, Au-Pt and TiO_2-Pt (under UV light of 200 mW/cm^2) motors spinning nearby SiO_2-Au Janus microspheres.

Video S7: SiO_2-Pt micromotors spinning an oil droplet (dibutyl phthalate).

References

1 B. R. Martin, D. J. Dermody, B. D. Reiss, M. Fang, L. A. Lyon, M. J. Natan and T. E. Mallouk, *Adv. Mater.*, 1999, **11**, 1021–1025.
2 DanV. Goia and E. Matijević, *Colloids and Surfaces A: Physicochemical and Engineering Aspects*, 1999, **146**, 139–152.
3 K. Baumgarten and B. P. Tighe, *Soft Matter*, 2017, **13**, 8368–8378.
4 T. R. Kline, J. Iwata, P. E. Lammert, T. E. Mallouk, A. Sen and D. Velegol, *J. Phys. Chem. B*, 2006, **110**, 24513–24521.
5 C. Liu, C. Zhou, W. Wang and H. P. Zhang, *Phys. Rev. Lett.*, 2016, **117**, 198001.
6 W. Wang, W. Duan, A. Sen and T. E. Mallouk, *Proc. Natl. Acad. Sci. U.S.A.*, 2013, **110**, 17744–17749.
7 R. Pethig, *Biomicrofluidics*, 2010, **4**, 022811.
8 L. Alvarez, M. A. Fernandez-Rodriguez, A. Alegria, S. Arrese-Igor, K. Zhao, M. Kröger and L. Isa, *Nat Commun*, 2021, **12**, 4762.
9 X. Yang, S. Johnson and N. Wu, *Advanced Intelligent Systems*, 2019, **1**, 1900096.
10 V. N. Shilov, A. V. Delgado, F. Gonzalez-Caballero and C. Grosse, *Colloids and Surfaces A: Physicochemical and Engineering Aspects*, 2001, **192**, 253–265.
11 F. Ma, X. Yang, H. Zhao and N. Wu, *Phys. Rev. Lett.*, 2015, **115**, 208302.
12 M. Wei, C. Zhou, J. Tang and W. Wang, *ACS Appl. Mater. Interfaces*, 2018, **10**, 2249–2252.
13 M. M. Gauthier and ASM International, Eds., *Engineered materials handbook*, ASM International, Materials Park, OH, Desk ed., 1995.
14 A. Rashidi and C. L. Wirth, *The Journal of Chemical Physics*, 2017, **147**, 224906.